J Biosci (2024)49:85
DOI: 10.1007/s12038-024-00465-4

Phosphorylation mapping of laminin γ1-chain: Kinases, functional interaction sequences, and phosphorylation-interfering cancer mutations

Panagiota-Angeliki Galliou[1]*, Kleio-Maria Verrou[2], Nikolaos A Papanikolaou[1] and George Koliakos[1]

[1]*Laboratory of Biological Chemistry, Medical School, Aristotle University of Thessaloniki, 54124 Thessaloniki, Greece*

[2]*Center of New Biotechnologies & Precision Medicine, National and Kapodistrian University of Athens, Medical School, 11527 Athens, Greece*

**Corresponding author (Email, ag.gal.work@gmail.com)*

MS received 18 September 2022; accepted 18 July 2024

We computationally predicted all phosphorylation sites in the sequence of the human laminin γ1-chain (LAMC1), and computationally identified, for the first time, all kinases for experimentally observed phosphorylated residues of the LAMC1 and all missense deleterious LAMC1 mutations found in different cancer types that interfere with LAMC1 phosphorylation. Also, we mapped the above data to all the biologically functional interaction sequences of the LAMC1. Five kinases (CKII, GPCRK1, PKA, PKC, and CKI) are most enriched for LAMC1 phosphorylation, and the significance of ecto-kinases in this process was emphasized. PKA and PKC targeted more residues inside and close to functional interaction sequences compared with other kinases and in the functional interaction sequence RPESFAIYKRTR. Most phosphorylation-interfering mutations were found in cutaneous melanoma and uterine endometrioid carcinoma. The mutation R255H interfered with the experimentally observed phosphorylation of LAMC1 inside the functional interaction sequence TDIRVTLNRLNTF, while the mutations S181Y and S213Y interfered with the experimentally observed phosphorylation of LAMC1 outside the functional interaction sequences. Mutations R359C,H, R589H, R657C,H, R663I,G, and T1207 interfered with the predicted phosphorylation inside or close to the functional interaction sequences, whereas other mutations interfered outside. PKA- and PKC-predicted phosphorylation was mostly interfered with by mutations inside functional interaction sequences. Phosphorylation-interfering mutations and functional interaction sequences were suggested to promote specific cancer types or cancer progression in general.

Keywords. Cancer mutations; functional interaction sequences; kinases; LAMC1; laminin γ1-chain; phosphorylation

1. Introduction

Laminin-111 is a fundamental extracellular matrix (ECM) glycoprotein, mainly expressed in adult epithelial tissues. It binds to other ECM laminin isoforms and molecules and plays an important role in cell adhesion, migration, differentiation, signaling, and polarization (Streuli 1995; Hohenester and Yurchenco 2013). The γ1-chain of laminin (LAMC1) synthesizes 11 of the 15 laminin isoforms (Timpl *et al*. 1979; Aumailley *et al*. 2005) and is involved in prion disease (Machado *et al*. 2012).

Biologically functional interaction sequences are protein regions with significant functional roles such as molecular interactions, substrate binding, and chemical reaction catalysis. There are multiple known biologically

Supplementary Information: The online version contains supplementary material available at https://doi.org/10.1007/s12038-024-00465-4.

functional interaction sequences in LAMC1 that mainly bind molecules such as integrin and nidogen and adhere to various types of cells, including cancer (Liesi *et al*. 1989; Mayer *et al*. 1993; Pöschl *et al*. 1994; Nomizu *et al*. 1997; Ponce *et al*. 1999; Powell *et al*. 2000; Kuratomi *et al*. 2002; Kasai *et al*. 2007). For instance, in LAMC1, the functional interaction sequences SLLSIINDLLEQ and TNAVGYSVYSIS highly promote neural cell growth. Also, the 58 residue-long functional interaction sequence γIII4 (TNCPTGTTGKRCELCDDGYFGDPLGRNGP VRLCRLCQCSDNIDPNAVGNCNRLTGECL), with its essential heptapeptide NIDPNAV, only binds nidogen. Furthermore, AFSTLEGRPSAY and FDPE-LYRSTGHGGH bind endothelial cells and have high angiogenic activity *in vivo*. SETTVKYVFRLHE has high angiogenic activity *in vivo,* binds endothelial cells, neural cells, salivary gland cells, and three cancer cell lines (HT-1080, B16-F10, and PC12), and promotes neurite outgrowth. NDPKVLKSYYYAISDFAVGGR has high angiogenic activity *in vivo,* binds endothelial cells, neural cells, salivary gland cells, the cancer cell lines HT-1080, B16-F10, and NG108, and promotes the growth of the PC12 cancer cell line. RPESFAIYKRTR only binds two cancer cell lines (HT-1080 and B16-F10). Both SFSFRVDRRDTR and TSTEAYNLLLRT bind the cancer cell lines HT-1080 and B16-F10 and promote the growth of neural cells. TDIRVTLNRLNTF binds endothelial cells, salivary gland cells, and the PC12 cancer cell line.

Furthermore, a few functional interaction sequences of LAMC1 not only bind cancer cell lines but also promote their growth and metastasis. FQKLLNNLTSI-KIRGTYSER binds integrin α2β1, endothelial cells, neural cells, salivary gland cells, and the cancer cell lines HT-1080, B16-F10, and NG108, and promotes the growth of the cancer cell line PC12 as well. KAFDI-TYVRLKF binds neural cells, promotes the growth of endothelial and salivary gland cells, binds the cancer cell lines HT-1080, B16-F10, and NG108, and promotes the growth of the cancer cell line PC12, the metastasis of the cancer cell line B16-F10, and the formation of amyloid-like fibrils *in vivo*. Amyloid fibrils are formed by the attachment of multiple misfolded protein aggregates in the ECM. Besides their physiological role, they compromise the healthy functioning of tissues and organs and are therefore associated with several diseases such as Alzheimer's and Parkinson's (Fowler *et al*. 2007; Eisenberg and Jucker 2012).

Phosphorylation and dephosphorylation regulate protein function by switching protein functional interaction sequences on and off (Ashcroft *et al*. 1999; Olsen *et al*. 2006). Ecto-kinases are located on the cell surface and have their catalytic site outside the cell utilizing the ATP of the ECM (Imada 1988). Ecto-kinase activity has been demonstrated in multiple cells (Ehrlich *et al*. 1986; Dusenbery *et al*. 1988; Babinska *et al*. 1996), while several transmembrane and ECM proteins, including laminin-111, are known to be ecto-phosphorylated (Apasov *et al*. 1996; Geberhiwot and Skoglund 1997; Seger *et al*. 1998; Zimina *et al*. 2007; Yalak and Vogel 2015). Protein kinase A (PKA), protein kinase C (PKC), and casein kinase II (CKII) have been reported to ecto-phosphorylate laminin-111, affecting its biological properties, such as self-assembly, and influencing its functions, like heparin binding and cell binding (Hogan *et al*. 1995; Kondrashin *et al*. 1999; Koliakos *et al*. 2000; Koliakos *et al*. 2001; Bohana-Kashtan *et al*. 2005; Trachana *et al*. 2005).

LAMC1 is part of the important laminin-111 protein and has multiple interaction sequences with different functional roles. Even though the functional interaction sequences in LAMC1 have been identified, there is little knowledge regarding their regulation by phosphorylation physiologically or in diseases. Therefore, we utilized bioinformatic tools to map the phosphorylation of LAMC1 and understand the regulation of its functional interaction sequences by specific kinases in healthy tissue in comparison with cancerous tissue. Our *de novo* results will provide significant aid to the scientific community as they increase the efficiency of *in vitro* experiments. In summary, we predicted all possible phosphorylation sites in LAMC1 using kinase binding motifs, which, in turn, led to the identification, for the first time, of all computationally identified kinases for each experimentally observed phosphorylated residue; it also predicted new putative phosphorylations. Also, we identified all point mutations found in cancer that interfere with the experimentally observed phosphorylated residues and which could interfere with the predicted phosphorylations in LAMC1. Finally, we generated an integrated phosphorylation–mutation map of LAMC1 that aims to be a useful analytic tool for the design of future targeted experiments.

2. Methods

2.1 *Sequence retrieval*

The sequence of LAMC1 was extracted in FASTA format (The Uniprot Consortium 2017, code P11047), which has an annotation score of 5 out of 5 and is saved as a .txt document (links in supplementary table 1).

2.2 *Recording of LAMC1 functional interaction sequences*

Functional interaction sequences in LAMC1 were recorded as previously (Galliou *et al*. 2019). An extensive literature search in PubMed (Canese and Weis 2002) was conducted to record all functional interaction sequences with a biological function, regardless of the cell type and experimental method used for identification. Overlapping functional interaction sequences were considered as one sequence. The literature-derived functional interaction sequences were matched to the consensus sequence of LAMC1 and their percentage identity was assessed by a similarity score (similarity score = number of identical residues between a literature-derived functional interaction sequence and an identified functional interaction sequence in the consensus sequence of LAMC1/length of the functional interaction sequence). A similarity score of 100% signifies two identical sequences, whereas a score of 0% signifies two completely different sequences. Functional interaction sequences in LAMC1 were saved in a .txt document (links in supplementary table 1) with a specific format (Galliou and Verrou 2019). Also, the sequence and function of recorded functional interaction sequences in LAMC1 were presented as a functional interaction sequence review (supplementary table 2).

2.3 *Experimentally observed phosphorylated residues*

The experimentally observed phosphorylated residues were recorded as before (Galliou *et al*. 2019). We scanned PhosphoSitePlus (Hornbeck *et al*. 2015) using the high-throughput papers (HTP) option to retrieve the phosphorylated LAMC1 residues that were experimentally assigned only through proteomic mass spectrometry. The retrieved residues were confirmed by a thorough literature search and saved in a .txt document (links in supplementary table 1) using a specific format (Galliou and Verrou 2019).

2.4 *Kinase motifs*

Recognition motifs of kinases indicate the sub-sequences in proteins that are required for kinase binding and phosphorylation, and were recorded as previously described (Galliou *et al*. 2019). A serine/threonine kinase/phosphatase motif query on Phosphomotif Finder (Amanchy *et al*. 2007) about all three chains of laminin-111 – LAMA1 (The Uniprot Consortium 2017, code P25391-1), LAMB1 (The Uniprot Consortium 2017, code P07942), and LAMC1 – resulted in all recognition motifs of all putative kinases that could phosphorylate LAMC1. The results were merged, sorted, and filtered in Excel to contain only kinases, and were saved in a .txt document (links in supplementary table 1) using a specific format (Galliou and Verrou 2019).

2.5 *LAMC1 mutations in cancer patients*

All mutations in the LAMC1 gene and protein found in cancer patients in all cancer types were retrieved from CBioPortal (Cerami *et al*. 2012; Gao *et al*. 2013), which uses Uniport for protein sequences, and saved in a .xlsx (Excel) document (links in supplementary table 1).

2.6 *In silico study of LAMC1 phosphorylation*

The PhosphoKin tool (Galliou and Verrou 2019) was used to study the phosphorylation of LAMC1. This tool uses as input four .txt files: the LAMC1 sequence, the functional interaction sequences, the experimentally observed phosphorylated resuidues, and the recognition motifs of kinases (links in supplementary table 1). The tool searched the recognition motifs of kinases against the LAMC1 sequence and identified the exact sub-sequences in LAMC1 that could be recognized and bound by kinases and, thus, computationally predicted all phosphorylation sites and phosphorylated residues. Also, by combining the computationally predicted phosphorylation sites in LAMC1 with the experimentally observed phosphorylated residues, it computationally identified all putative kinases for each experimentally observed phosphorylated residue in LAMC1. Then, it classified the experimentally observed and predicted phosphorylated residues into three categories: inside the functional interaction sequences, outside the functional interaction sequences, and close within six residues in proximity to functional interaction sequences.

Furthermore, we modified PhosphoKin (supplementary table 1) to also take as input an .xlsx document with the cancer mutations (supplementary table 1). Using the LAMC1 mutations file as input in PhosphoKin, we identified all missense cancer point

mutations in LAMC1 that interfered with the experimentally observed and predicted phosphorylation sites of LAMC1 (supplementary table 1). Missense cancer point mutations interfering with LAMC1 phosphorylation were considered those that were located either directly on predicted phosphorylated residues or on required residues for kinase binding to phosphorylation sites according to the kinases' recognition motifs. The missense cancer point mutations interfering with LAMC1 phosphorylation were categorized by cancer type, location relative to functional interaction sequences (inside, outside, and close within six residues proximity), and the classified mutation functional impact according to CBioPortal (tolerated and deleterious).

2.7 *Mapping LAMC1 phosphorylation sites and missense point mutations in cancer*

Using different styling formats we illustrated the recorded functional interaction sequences as well as the experimentally observed and predicted phosphorylated residues in the LAMC1 sequence, as previously described (Galliou *et al*. 2019). Also, we illustrated all missense point mutations found in all types of cancer, generating an integrated phosphorylation–mutation map of LAMC1 (supplementary figure 1), which was very useful for further analysis. Briefly, in the integrated phosphorylation–mutation map of LAMC1, the recorded functional interaction sequences were marked with boldface, the experimentally observed phosphorylated residues were marked in red-colored letters, and the predicted phosphorylation sites were highlighted in yellow. The interaction of LAMC1 residues with different kinases is described with a list of interaction rows, where each interaction row corresponds to a single kinase. The absence of interaction is displayed with '-', binding of a residue with 'X', and phosphorylation of a residue with 'P'. Also, the residues found mutated in cancer were underlined and their missense mutation(s) were written above them in blue color.

3. Results

3.1 *Integrated phosphorylation–mutation map of LAMC1*

We mapped the literature-derived, functional interaction sequences of LAMC1, the experimentally observed and predicted phosphorylated residues, and all missense point mutated residues found in different cancers (supplementary figure 1). Twenty functional interaction sequences, 22 experimentally observed phosphorylated residues (Stokes 2007; Possemato 2008; Rush 2008; Gu 2009; Ren 2009; Blasius *et al*. 2011; Rigbolt *et al*. 2011; Rikova 2011; Zhou 2011; Mertins *et al*. 2014, 2016), 181 predicted phosphorylated residues, and 72 missense point mutations in cancer were mapped. Of the 181 predicted phosphorylated residues, 161 were identified for the first time.

3.2 *Computationally identified kinases for experimentally observed phosphorylated residues in LAMC1*

Twenty-two LAMC1 phosphorylated residues have been experimentally found and 183 were predicted. All residues were sorted according to their location relative to functional interaction sequences. Of the experimentally observed phosphorylated residues, 7 were located inside functional interaction sequences, 2 were close to within six residues of functional interaction sequences, and 13 were outside functional interaction sequences (table 1). Of the predicted phosphorylated residues, 43 were located inside functional interaction sequences, 26 close to within six residues, and 141 outside (supplementary table 3). We found that 31.8% of experimentally observed phosphorylations and 23.5% of predicted phosphorylations were located inside functional interaction sequences, while 9.1% of experimentally observed phosphorylations and 14.2% of predicted phosphorylations were located close to functional interaction sequences.

Using the recognition motifs of kinases we computationally predicted the exact sub-sequences in LAMC1 that could be bound and phosphorylated by each kinase, and for the first time, we computationally identified all putative kinases for 20 of the 22 experimentally observed phosphorylated residues LAMC1 (table 1). Experimentally observed LAMC1 phosphorylations were inside or close to four functional interaction sequences. The experimentally observed phosphorylated residue T258 is located inside TDIRVTLNRLNTF, and the kinases PKC, CKII, CaMKII, CaMKII alpha, CaMKIV, and Chk1 were identified as its putative kinases. The fact that T258 is phosphorylated by Chk1 *in vitro* (Blasius *et al*. 2011) demonstrates the validity of our predictive approach. Furthermore, T1529 is close to SLLSIINDLLEQ,

Table 1. Computationally identified kinases for the experimentally observed phosphorylated residues in LAMC1

Nos.	Phosphorylated residue	Computationally identified kinases	Location of residue relative to functional interaction sequences			
			Inside	Close	Outside	Functional interaction sequence
1	S4	PKA†[1], PKC†[2], GPCRK1			✔	
2	S159	PKA†[1], PKC†[2], CaMKII, BARK-1, MAPKAPK2	✔			RPESFAIYKRTR[a]
3	T166	PKA†[1], PKC†[2], CKII†[3]	✔			RPESFAIYKRTR[a]
4	S181	GPCRK1, MAPKAPK2			✔	
5	T196	CKII†[3]			✔	
6	S210	CKII†[3], CKI			✔	
7	T216	-		✔		AFSTLEGRPSAY[b]
8	T258	PKC†[2], CKII†[3], CaMKII, CaMKII-alpha, CaMKIV, Chk1	✔			TDIRVTLNRLNTF[b,c,d]
9	S272	PKA†[1], CKII†[3], GPCRK1	✔			NDPKVLKSYYYAISDFAVGGR[a,b,c,d,e,f]
10	Y273	-	✔			NDPKVLKSYYYAISDFAVGGR[a,b,c,d,e,f]
11	Y274	JAK2, Src	✔			NDPKVLKSYYYAISDFAVGGR[a,b,c,d,e,f]
12	Y275	Src	✔			NDPKVLKSYYYAISDFAVGGR[a,b,c,d,e,f]
13	Y413	Src			✔	
14	T1127	BARK1			✔	
15	S1149	CKII†[3], CKI			✔	
16	S1275	CKII†[3], CKI, GPCRK1, GSK-3, PDK, ERK1, ERK2, CDK5, MAPKAPK2			✔	
17	Y1307	ALK, EGFR, JAK2, Src			✔	
18	S1493	DNA-PK, ATM			✔	
19	T1529	BARK1		✔		SLLSIINDLLEQ[e]
20	T1541	GPCRK1			✔	
21	S1559	PKA†[1], PKC†[2], CKII†[3], CKI, PKC-Epsilon, CaMKII, CaMKIV, Chk1			✔	
22	S1605	CKII†[3], GPCRK1			✔	

Kinases with reported ecto-kinase activity are annotated with the symbol '†' and their references are denoted with the exponent numbers in brackets ([1] Kondrashin *et al*. 1999; [2] Hogan *et al*. 1995; [3] Bohana-Kashtan *et al*. 2005). Lowercase letters symbolize the functionality of interaction sequences. a: cell adhesion to cancer cell lines (fibrosarcoma HT1080, melanoma B16F10); b: cell adhesion (endothelial cells); c: cell adhesion (salivary gland-HSG cells); d: cell adhesion to a cancer cell line (pheochromocytoma PC12); e: cell adhesion (neural cells); f: cell adhesion to a cancer cell line (neuroblastoma NG108).

which highly promotes neurite outgrowth, with only BARK1 as a putative kinase. Inside NDPKVLK SYYYAISDFAVGGR, the residue S272 is experimentally phosphorylated with kinases PKA, CKII, and GPCRK1, and the residues Y274 and Y275 with Src as their only putative kinase. Inside RPESFAIYKRTR, the residue T166 is experimentally phosphorylated with kinases PKA, PKC, and CKII, and the residue S159 with PKA and PKC is included in its kinases. Thus, PKA and PKC that have ecto-phosphorylating activity target the functional interaction sequence RPESFAIYKRTR, which binds to fibrosarcoma HT1080 and melanoma B16F10 cancer cell lines.

3.3 *Enriched kinases in the phosphorylation of LAMC1*

The LAMC1 residues that were computationally identified for each kinase were counted to investigate their significance (figure 1). CKII was computationally identified for nine, while GPCR1 for six, and PKA and PKC for five experimentally observed phosphorylated residues (figure 1A). CKI and Src were identified for four experimentally observed phosphorylated residues, while the remaining kinases were for less than four residues. Moreover, CKII followed by the kinases GPCRK1, PKA, PKC, and CKI had the highest number of predicted phosphorylated residues, which were

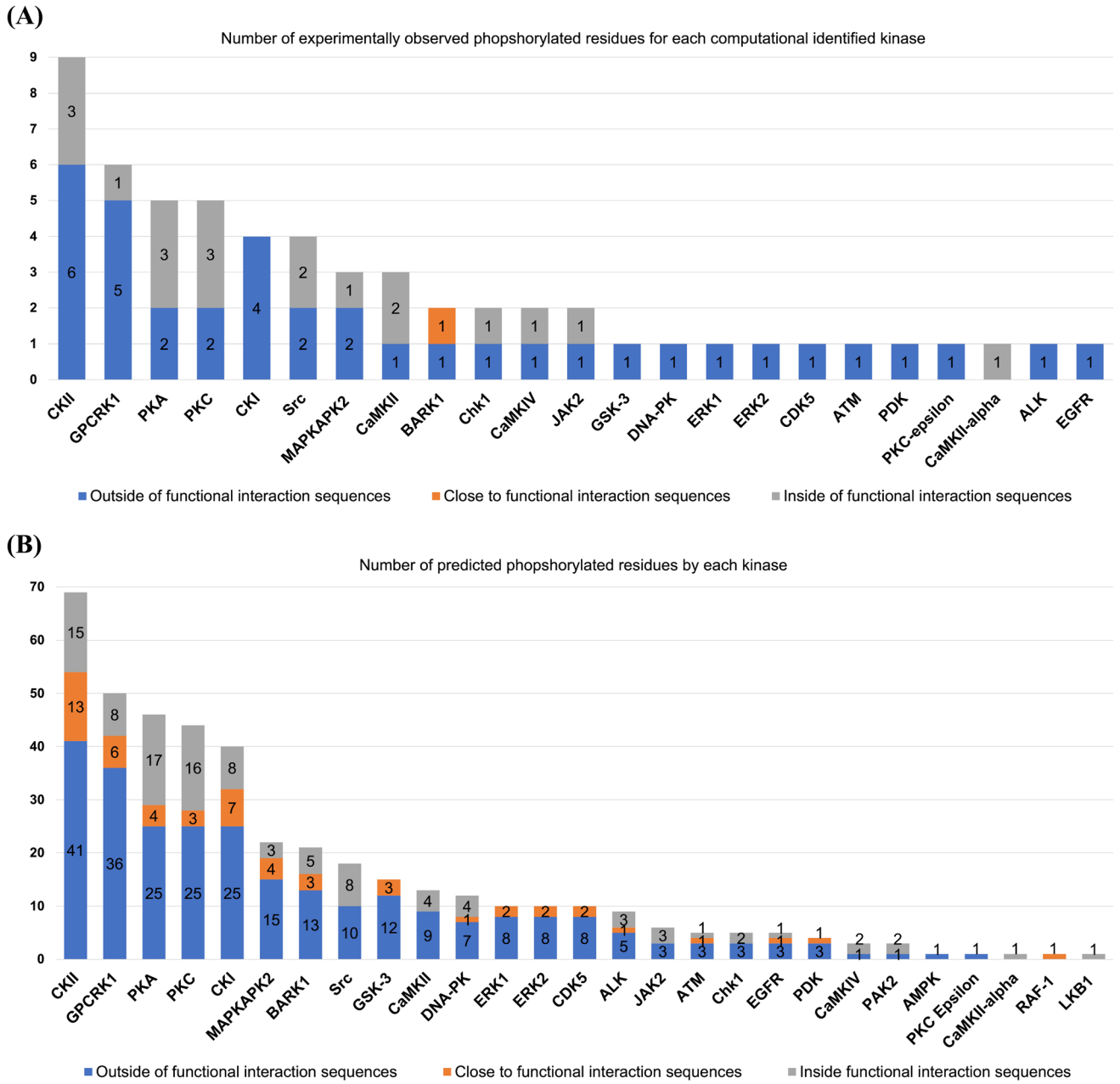

Figure 1. Number of phosphorylated residues in LAMC1 for each kinase. (**A**) Number of experimentally observed phosphorylated residues for each computationally identified kinase. (**B**) Total number of predicted phosphorylated residues by each kinase. Supplementary table 2 shows the exact phosphorylated residues for each kinase relative to functional interaction sequences.

60, 50, 46, 44, and 40 residues, respectively, (figure 1B). Therefore, five kinases (CKII, GPCRK1, PKA, PKC, CKI) were found enriched for LAMC1 phosphorylation.

Furthermore, we investigated the activity of the kinases relative to the LAMC1 functional interaction sequences (figure 1). All experimentally observed phosphorylated target residues of CKI and most of CKII and GPCR1 were outside functional interaction sequences, while most target residues of PKA and PKC were inside functional interaction sequences (figure 1a). Even though the predicted phosphorylated target residues of CKII, GPCRK1, CKI, PKA, and PKC were mostly outside functional interaction sequences, PKA and PKC had a high number of predicted phosphorylated residues inside and close to functional interaction sequences (figure 1b). Therefore, of the five enriched kinases in LAMC1 phosphorylation, PKA and PKC targeted more residues inside and close to functional

interaction sequences, whereas CKII, GPCRK1, and CKI targeted more residues outside functional interaction sequences.

3.4 *Deleterious missense point mutations interfering with LAMC1 phosphorylation in cancer*

We computationally identified all LAMC1 missense point mutations found in cancer that interfere with the experimentally observed and predicted phosphorylations in LAMC1 (supplementary table 1). In total, 96 mutations interfered with LAMC1 phosphorylation in 35 cancer types, 54 of which were deleterious and 42 were tolerated (supplementary table 4A). Most mutations were localized outside functional interaction sequences, while most mutations inside and outside functional interaction sequences were deleterious (supplementary table 4A).

The 54 deleterious and phosphorylation-interfering cancer mutations were found in 23 different cancer types (figure 2). They were mostly found in skin cancers, specifically in cutaneous melanoma, and in cancers of the female reproductive system, specifically in uterine endometrioid carcinoma. Most deleterious LAMC1 mutations in cutaneous melanoma were located inside or close to functional interaction sequences, whereas most mutations in uterine endometrioid carcinoma were localized outside LAMC1 functional interaction sequences. Eight LAMC1 mutations were found generally in lung cancer and all were outside functional interaction sequences.

3.4.1 *Cancer mutated LAMC1 residues S181, S213, R255 interfere with experimentally observed phosphorylation in LAMC1:* The LAMC1 residue S181 is located outside functional interaction sequences and was found mutated to tyrosine in one sample (table 2) in lung squamous cell carcinoma (figure 2). Thus, the LAMC1 cancer mutation S181Y interferes with the residue's experimentally observed phosphorylation by the kinases GPCRK1 and MAPKAPK2 (table 2). The

	Cancer types	Total mutations	Location to active sites: Inside	Close	Outside	Mutated Resides
Brain	Glioblastoma Multiforme	1	0	0	1	S213
	Astrocytoma	1	1	0	0	R657
Esophagus and stomach	Stomach Adenocarcinoma	2	1	1	0	R255 L639
	Esophagogastric Adenocarcinoma	1	1	0	0	R657
Female reproductive system	Cervical Squamous Cell Carcinoma	1	0	0	1	D1555
	Uterine Carcinosarcoma/ Uterine Malignant Mixed Mullerian	1	0	0	1	A1269
	Uterine Endometrioid Carcinoma	9	4	0	5	R255 R663 T1207 S436 S605 T746 R1121 R1143
	Uterine Serous Carcinoma/ Uterine Papillary Serous Carcinoma	2	2	0	0	R589 T737
Head and neck	Head and Neck Squamous Cell Carcinoma	1	1	0	0	D587
Kidney	Papillary Renal Cell Carcinoma	1	0	0	1	E711
Large intestine	Colon Adenocarcinoma	1	0	0	1	S436
	Colorectal Adenocarcinoma	2	2	0	0	R359 R657
	Rectal Adenocarcinoma	1	1	0	0	R663
Liver	Hepatocellular Adenoma	3	0	1	2	K1507 E711 T1603
Lung	Lung Adenocarcinoma	3	0	0	3	E294 G313 R677
	Lung Squamous Cell Carcinoma	4	0	0	4	P72 S181 S768
	Small Cell Lung Cancer	1	0	0	1	S446
Male reproductive system	Prostate Adenocarcinoma	2	1	1	0	R589 Y854
Skin	Melanoma	2	1	0	1	R359 S1598
	Cutaneous Melanoma	10	6	1	3	E226 T252 R359 P616 D808 P449 P713
	Desmoplastic Melanoma	3	1	0	2	R359 S486 E535
	Lentigo Maligna Melanoma	1	0	0	1	P449
Urinary system	Bladder/Urinary Tract	1	1	0	0	T1207
	Total	54	23	4	27	37

Figure 2. The number of LAMC1 deleterious point mutations and LAMC1 deleterious mutated residues that interfered with the phosphorylation of LAMC1, categorized by cancer type and location relative to functional interaction sequences in LAMC1. Data are presented as a heatmap, with different color intensities corresponding to different numbers of mutations. The red-shaded cells display the number of total mutations and the number of mutations inside, close, and outside of functional interaction sequences. Cancer-mutated residues are indicated with green-shaded cells: light green indicates that the residue was found mutated in one sample, medium-shaded green indicates that the residue was found mutated in two samples, and dark green indicates that the residue was found mutated in three samples.

Table 2. Deleterious cancer point mutated LAMC1 residues interfering with the phosphorylation of experimentally observed and predicted phosphorylated residues in LAMC1

		Phosphorylation interference		Phosphorylated residue location relative to functional interaction sequences	
Mutated residue	Number of times mutated	Phosphorylated residue	Computational identified kinase(s)	Location	Functional interaction sequence
For experimentally observed phosphorylated residues					
R255H	2	T258	PKC, CaMKII, CaMKIV, Chk1, CaMKII-alpha	Inside	TDIRVTLNRLNTF
S181Y	1	S181	GPCRK1, MAPKAPK2	Outside	–
S213Y	1	S210	CKI	Outside	–
For predicted phosphorylated residues					
R359C,H	6	T361	PKA, PKC	Inside	FDPELYRSTGHGGH
R657C,H	3	T659	PKA, PKC	Inside	LTPFEFQKLLNNLTSIKIRGTYSER
R663I,G	3	S661	PKA, PKC	Inside	LTPFEFQKLLNNLTSIKIRGTYSER
R589H	2	S591	PKA, PKC	Inside	SFSFRVDRRDTR
T1207M	2	T1207	CKII, BARK1	Inside	TSTEAYNLLLRT
		T1203	GPCRK1	Close	TSTEAYNLLLRT
P72Q	2	T68	GPCRK1	Outside	–
		T71	GSK-3, ERK1, ERK2, CDK5	Outside	–
S436Y,F	2	S436	CKII, GPCRK1	Outside	–
P449L	2	S450	DNA-PK	Outside	–
E711V,K	2	T712	BARK1	Outside	–
P713S,H	2	T712	GSK-3, ERK1, ERK2, CDK5	Outside	–

This table displays all cancer mutated residues that interfere with the phosphorylation of the experimentally observed phosphorylated residues; for the interference of predicted phosphorylations, only the cancer mutated residues that are found in more than one sample are displayed.

LAMC1 residue S213 is outside functional interaction sequences and was found mutated to tyrosine in one sample in glioblastoma multiforme (figure 2). This residue is necessary for the experimentally observed phosphorylation of the LAMC1 residue S210 by its only kinase CKI. Therefore, cancer mutation S213Y interferes with the experimentally observed phosphorylation of residue S210 by CKI. The LAMC1 residue R255 is located inside the functional interaction sequence TDIRVTLNRLNTF and was found mutated to histidine in stomach adenocarcinoma and uterine endometrioid carcinoma. This residue is necessary for the experimentally observed phosphorylation of T258 by its putative kinases PKC, CaMKII, CaMKII-alpha, CaMKIV, and Chk1 (table 2). Thus, the enriched R255H cancer mutation interferes with the experimentally observed phosphorylation of T258 and could have a general role in cancer progression.

3.4.2 *Cancer-mutated LAMC1 residues R359, R657, R663, and R589 interfere with predicted phosphorylation by PKA and PKC inside functional interaction sequences:* The LAMC1 residue R359 is located inside the functional interaction sequence FDPELYRSTGHGGH and it is the most enriched LAMC1 mutated residue in cancer (figure 2; table 2), as it was found mutated in six samples in total, five times to cysteine and once to histidine (data not shown). Also, it was found to be enriched in melanoma tumors, such as cutaneous melanoma (three samples), desmoplastic melanoma (one sample), melanoma (one sample), and colorectal adenocarcinoma (one sample). This residue is necessary for the predicted phosphorylation of residue T361 by PKA and PKC, and thus the enriched cancer mutation R359C,H interferes with the predicted phosphorylation of T361 by PKA and PKC inside the functional interaction sequence FDPELY RSTGHGGH.

LAMC1 residues R657 and R663 are located inside the functional interaction sequence LTPFEFQ KLLNNLTSIKIRGTYSER and were both found mutated three times in cancer. The cancer-mutated residue R657 was found to have a general role in cancer as it was mutated in esophagogastric

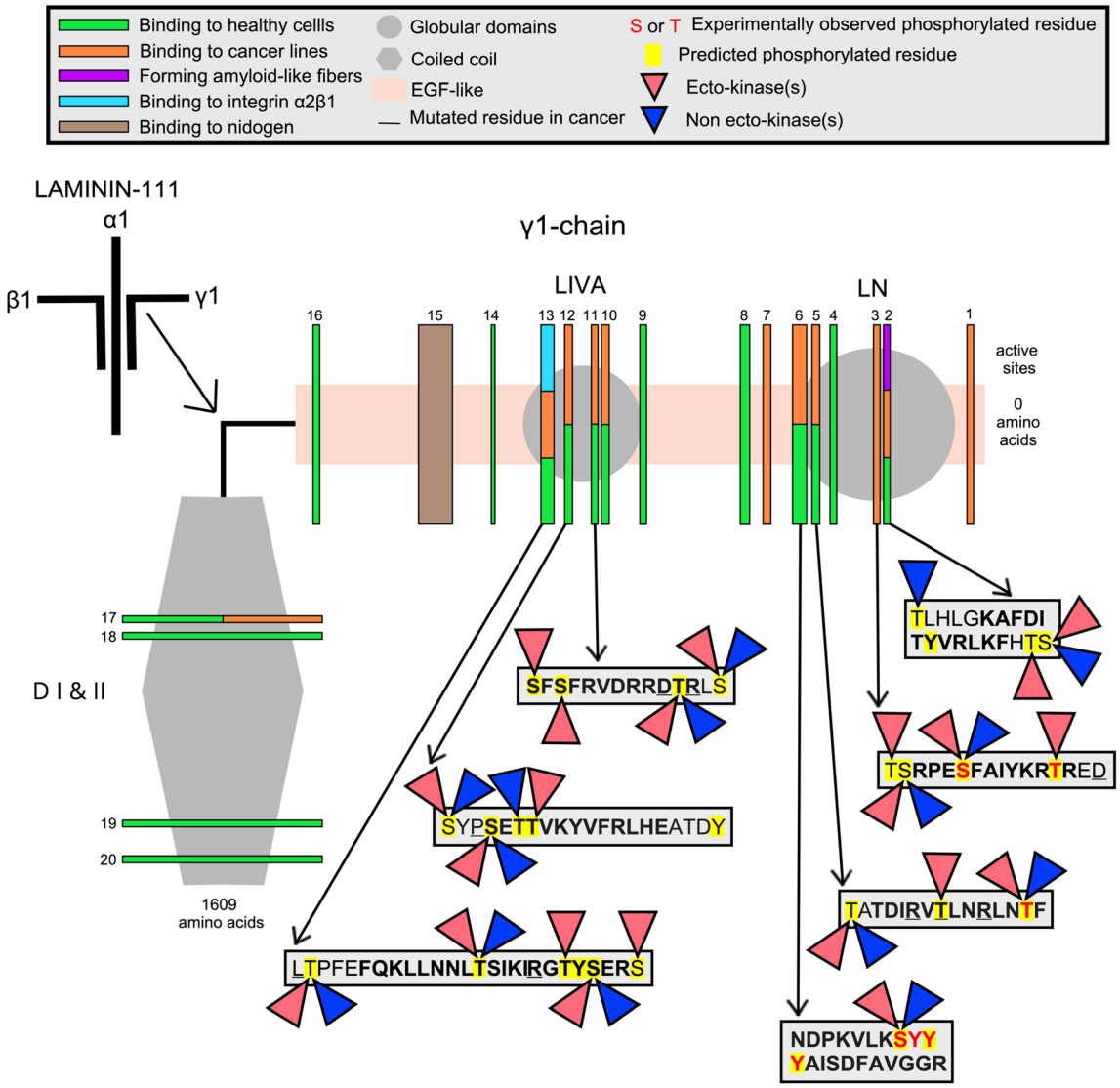

Figure 3. Functional interaction sequences in the structure of LAMC1, their function, and emphasis in six functional interaction sequences. The structure of LAMC1 consists of EGF-like areas, the LN and LIVA that are globular domains, and the DI & II domain that intertwines with the rest of the laminin-111 chains. Rectangles are used to depict the 20 functional interaction sequences in LAMC1. The size of each functional interaction sequence is proportional to its length. Interaction sequences are colored variously to correspond to their separate functions, according to literature. Different functions, according to literature, are displayed with distinct coloring of the rectangles; green, orange, cyan, and brown correspond to healthy cells, cancer cell lines, integrin α2β1, and nidogen binding, respectively, whereas purple corresponds to amyloid-like fiber formation. Functional interaction sequences with more than one function are multi-colored. The order of the colors is random and signifies the function of the whole functional interaction sequence. Emphasis was given to six functional interaction sequences, for which the experimentally observed and predicted phosphorylated residues and the deleterious cancer mutated residues are displayed. Red indicates an experimentally observed phosphorylation, while yellow highlights and underlined letters show a predicted phosphorylated residue and a mutated residue, respectively. The kinase(s) of phosphorylated amino acids are shown with triangles: pink triangles indicate kinases with known ecto-phosphorylation activity, whereas blue triangles indicate kinases that do not have an ecto-phosphorylation activity.

adenocarcinoma (one sample), astrocytoma (one sample), and colorectal adenocarcinoma (one sample), whereas the cancer-mutated residue R663 was found enriched in uterine endometrioid carcinoma as it was found mutated in two samples of uterine endometrioid carcinoma and one of rectal adenocarcinoma. R657 was necessary for the predicted phosphorylation of T659 and R663 for the predicted phosphorylation of

S661 by PKA and PKC (table 2). Thus, the enriched cancer mutations R657C,H, and R663I,G interfere with the predicted phosphorylations of PKA and PKC inside the functional interaction sequence LTPFEFQKLLNNLTSIKIRGTYSER.

The LAMC1 residue R589 is located inside the functional interaction sequence SFSFRVDRRDTR and was found to have a general role in cancer progression as it was found mutated twice, once in uterine papillary serous carcinoma and once in prostate adenocarcinoma. This residue is required for the predicted phosphorylation of S591 by PKA and PKC, and thus the enriched cancer mutation R589H interferes with the predicted phosphorylation of S591 by PKA and PKC inside the sequence SFSFRVDRRDTR.

The LAMC1 residue T1207 is located inside the functional interaction sequence TSTEAYNLLLRT and was found to have a general role in cancer progression, as it was mutated two times, once in uterine endometroid carcinoma and once in bladder/urinary tract cancer. This residue was predicted to be phosphorylated by CKII and BARK1 and it is required for the predicted phosphorylation of T1203 by GPCRK1. Thus, the enriched cancer mutation T1207M interferes with both the predicted phosphorylation of T1207 by CKII and BARK1 inside the sequence TSTEAYNLLLRT and the predicted phosphorylation of T1203 by GPCRK1.

3.4.3 *LAMC1 predicted phosphorylation interference by cancer-mutated residues outside functional interaction sequences:* The LAMC1 cancer mutation P72Q was found enriched in lung squamous cell carcinoma and could interfere with the predicted phosphorylation of LAMC1 residue T68 by GPCRK1 and residue T71 by GSK-3, ERK1, ERK2, and CDK5 (figure 2; table 2). The LAMC1 cancer mutation S436Y,F was found to have a general role in cancer progression as it was mutated in colon adenocarcinoma (one sample) and small cell lung cancer (one sample), and could interfere with the residue's predicted phosphorylation by CKII and GPCRK1. The LAMC1 cancer mutation P449L was enriched in melanoma in general, as it was mutated once in cutaneous melanoma and once in lentigo malignant melanoma, and it could interfere with the predicted phosphorylation of the LAMC1 residue S450 by DNA-PK. The LAMC1 cancer mutation E711V,K was found to have a general role in cancer progression, and the cancer mutation P713S,H was enriched in cutaneous melanoma, as the former was found mutated once in papillary renal cell carcinoma and once in hepatocellular adenoma, while the latter was found mutated in two samples of cutaneous melanoma. Both LAMC1 cancer mutations could interfere with the predicted phosphorylation of LAMC1 residue T712 by BARK1, GSK-3, ERK1, ERK2, and CDK5.

4. Discussion

Laminin-111, a crucial extracellular matrix (ECM) protein, plays a pivotal role in various cellular functions. Previous investigations by Galliou *et al.* (2019) and Verrou *et al.* (2019) delved into the phosphorylation dynamics of the α1-chain (LAMA1) and the β1-chain (LAMB1) of laminin, offering valuable insights for future research. In the current study, we aimed to extend this understanding by mapping the phosphorylation sites of LAMC1 to its functional interaction sequences and the mutations associated with cancer, to shed light on its regulatory mechanisms and potential implications for therapy.

We initially focused on identifying the functional interaction sequences within LAMC1, following a similar approach as with LAMA1 and LAMB1. It is worthwhile noting that while literature-derived functional interaction sequences were primarily based on mouse or rat sequences, their homology to human LAMC1 ensured their relevance. To bolster the confidence in our findings, we conducted a thorough assessment of sequence homology, revealing that all identified functional interaction sequences had significant similarity scores, with the majority surpassing the 90% threshold (supplementary figure 2). These sequences are compiled in our functional interaction sequences review (supplementary table 2), facilitating researchers in targeting specific regions of interest. Moreover, we acknowledge the cell-specific and potentially non-simultaneous functionality of these recorded functional interaction sequences.

Next, we employed kinase recognition motifs to computationally predict the kinases responsible for phosphorylating experimentally observed residues in LAMC1. While experimental validation is paramount, this computational approach aided in narrowing down the list of potential kinases, thus guiding the design of future experiments. Notably, we observed that most phosphorylated residues were serine and threonine residues, with a smaller fraction predicted to be tyrosine residues.

Furthermore, our analysis highlighted the enrichment of certain kinases in both experimentally observed and predicted phosphorylation events in LAMC1. Notably, three of the enriched kinases, PKA, PKC, and CKII,

exhibited distinct preferences in targeting residues within or near functional interaction sequences. Also, they were predicted to target interaction sequences with cancer cell binding function, such as TDIRVTLNRLNTF, SETTVKYVFRLHE, and KAFDITYVRLKF (supplementary figure 1), suggesting involvement in LAMC1 phosphorylation in cancer. Intriguingly, PKA, PKC, and CKII have been found upregulated in several cancers (Babiker *et al*. 2006; Wang *et al*. 2007) and they possess ecto-kinase activity, suggesting a potential role for extracellular phosphorylation events in modulating LAMC1 function. These findings parallel the observations made for LAMA1 and LAMB1, indicating a shared phosphorylation mechanism across the laminin-111 molecule.

Moreover, we investigated missense point mutations in LAMC1 associated with cancer and identified phosphorylation-interfering deleterious mutated residues for the first time. Of particular interest were mutations within or close to functional interaction sequences, which could potentially disrupt essential phosphorylation events crucial for proper function, thereby contributing to disease pathogenesis. Notably, certain mutations showed enrichment in specific cancer types, suggesting their potential involvement in disease progression, while others suggested their general involvement in cancer. Furthermore, taking into consideration the location of the enriched mutations in LAMC1, our findings suggest for the first time a role of phosphorylation interference in certain LAMC1 functional interaction sequences in specific cancer types and cancer progression in general. Specifically, our findings suggest phosphorylation interference of FDPELYRSTGHGGH in melanoma and cutaneous melanoma, of FQKLLNNLTSIKIRGTYSER in uterine endometrioid carcinoma and colorectal cancer, and of TDIRVTLNRLNTF, SFSFRVDRRDTR, and TSTEAYNLLLRT generally in cancer progression.

Considering our findings from the aspect of LAMC1 structure is of great importance for unraveling future research. Certain functional interaction sequences are within a few residues in proximity in the same LAMC1 domain. For example, SFSFRVDRRDTR, SETTVKYVFRLHE, and LTPFEFQKLLNNLTSIKIRGTY SER are located in the LIVA domain, while KAFDITYVRLKF, NDPKVLKSYYYAISDFAVGGR, RPESFAIYKRTR, and TDIRVTLNRLNTF are located in the LN domain (figure 3). The LN domain is part of the E4 fragment, which is essential for the self- and co-assembly of laminin-111 and is less stable against proteolysis that degrades it by 30% (Ott *et al*. 1982; Colognato and Yurchenco 2000). A proteolytic cleavage in any position in the fragile-structured LVIA and LN LAMC1 domains could compromise their function. Intriguingly, a cryptic site-revealing proteolytic cleavage has been identified in the β3-chain of laminin-5 (Giannelli 1997), and protease upregulation is known to drive disease progression in cancer (Rakashanda *et al*. 2012). Therefore, the above functional interaction sequences may represent cryptic sites revealed by proteolysis, compromising the physiological function of LAMC1 in cancer. Given the enrichment of PKA, PKC, and CKII in LAMC1 phosphorylation physiologically and in cancer and the fact that phosphorylation can trigger conformational changes in proteins (Ritz-Gold *et al*. 1980), these cryptic sites could be exposed by ecto-phosphorylation.

By elucidating the interplay between phosphorylation events, protein–protein interactions, and disease-associated mutations, we lay the groundwork for future research aimed at deciphering the complex biology of laminin-111 and its role in disease pathogenesis. These findings have the potential to inform the development of novel therapeutic strategies targeting ECM proteins and associated signaling pathways, with the ultimate goal of improving patient outcomes in various diseases, including cancer. In conclusion, our comprehensive analysis provides novel insights into the phosphorylation dynamics and mutational landscape of LAMC1, highlighting its potential implications in cancer biology. These findings pave the way for further investigations into the regulatory mechanisms of laminin-111 and its role in disease with *in vitro* experiments, such as site-directed mutagenesis and kinase assays, and have significant implications for therapeutic interventions.

Author contributions

P-A G took the lead in the literature search, data collection and analysis, design of tables and figures, and writing of the manuscript. K-M V and P-A G equally contributed to the development of the theoretical framework. NAP and P-A G equally contributed to the data interpretation and the reviewing of the manuscript. NAP provided critical feedback resulting in the final version of the manuscript. GK and NAP supervised the project.

Funding

This research did not receive any specific grant from funding agencies in the public, commercial, or not-for-profit sectors.

Declarations

Conflict of interest The authors declare no conflict of interest.

References

Amanchy R, Periaswamy B, Mathivanan S, *et al*. 2007 A curated compendium of phosphorylation motifs. *Nat. Biotechnol.* **25** 285–286

Apasov SG, Smith PT, Jelonek MT, *et al*. 1996 Phosphorylation of extracellular domains of T-lymphocyte surface proteins: constitutive serine and threonine phosphorylation of the T cell antigen receptor ectodomains. *J. Biol. Chem.* **271** 25677–25683

Ashcroft M, Kubbutat MHG and Vousden KH 1999 Regulation of p53 function and stability by phosphorylation. *Mol. Cell Biol.* **19** 1751–1758

Aumailley M, Bruckner-Tuderman L, Carter WG, *et al*. 2005 A simplified laminin nomenclature. *Matrix Biol.* **24** 326–332

Babiker AA, Ronquist G, Nilsson B, *et al*. 2006 Overexpression of ecto-protein kinases in prostasomes of metastatic cell origin. *Prostate* **66** 675–686

Babinska A, Ehrlich YH and Kornecki E 1996 Activation of human platelets by protein kinase C antibody: role for surface phosphorylation in homeostasis. *Am. J. Physiol. Heart Circulatory Physiol.* **271** H2134–H2144

Blasius M, Forment JV, Thakkar N, *et al*. 2011 A phosphoproteomic screen identifies substrates of the checkpoint kinase Chk1. *Genome Biol.* **12** R78

Bohana-Kashtan O, Pinna LA and Fishelson Z 2005 Extracellular phosphorylation of C9 by protein kinase CK2 regulates complement-mediated lysis. *Eur. J. Immunol.* **35** 1939–1948

Canese K and Weis S 2002 *PubMed: The bibliographic database* 2nd edition (Bethesda: National Center for Biotechnology Information) *https://www.ncbi.nlm.nih.gov/books/NBK153385/*

Cerami E, Gao J, Dogrusoz U, *et al*. 2012 The cBio Cancer Genomics Portal: an open platform for exploring multidimensional cancer genomics data. *Cancer Discov.* **2** 401–404

Colognato H and Yurchenco PD 2000 Form and function: the laminin family of heterotrimers. *Dev. Dyn.* **218** 213–234

Dusenbery KE, Mendiola JR and Skubitz KM 1988 Evidence for ecto-protein kinase activity on the surface of human neutrophils. *Biochem. Biophys. Res. Commun.* **153** 7–13

Ehrlich YH, Davis TB, Bock E, *et al*. 1986 Ecto-protein kinase activity on the external surface of neural cells. *Nature* **320** 67–70

Eisenberg D and Jucker M 2012 The amyloid state of proteins in human diseases. *Cell* **148** 1188–1203

Fowler DM, Koulov AV, Balch WE, *et al*. 2007 Functional amyloid – from bacteria to humans. *Trends Biochem. Sci.* **32** 217–224

Galliou PA and Verrou KM 2019 An in silico method for studying the phosphorylation in association to functional interaction sequences. *Aristotle Biomed. J.* **1** 48–59

Galliou PA, Verrou KM and Koliakos G 2019 Phosphorylation mapping of laminin α1-chain: kinases in association with functional interaction sequences. *Comput. Biol. Chem.* **80** 480–497

Gao J, Aksoy BA, Dogrusoz U, *et al*. 2013 Integrative analysis of complex cancer genomics and clinical profiles using the cBioPortal. *Sci. Signal* **6** pl1

Geberhiwot T and Skoglund G 1997 Cell surface and serum protein phosphorylation by U-937 cell ectoprotein kinases. *IUBMB Life* **4** 269–278

Giannelli G 1997 Induction of cell migration by matrix metalloprotease-2 cleavage of laminin-5. *Science* **277** 225–228

Gu T 2009 CST curation set: 6979; year: 2009; biosample/treatment: cell line, Molm 14/-; disease: acute myelogenous leukemia; SILAC: -; specificities of antibodies used to purify peptides prior to LCMS: pY antibodies used to purify peptides prior to LCMS: phospho-tyrosine mouse mAb (P-Tyr-100) cat#: 9411, PTMScan(R) phospho-Tyr motif (Y*) immunoaffinity beads cat#: 1991

Hogan MV, Pawlowska Z, Yang HA, *et al*. 1995 Surface phosphorylation by ecto-protein kinase C in brain neurons: a target for Alzheimer's beta-amyloid peptides. *J. Neurochem.* **65** 2022–2030

Hohenester E and Yurchenco PD 2013 Laminins in basement membrane assembly. *Cell Adh. Migr.* **7** 56–63

Hornbeck PV, Zhang B, Murray B, *et al*. 2015 PhosphoSitePlus, 2014: mutations, PTMs and recalibrations. *Nucleic Acids Res.* **43** D512–D520

Imada S 1988 Fibronectin phosphorylation by ecto-protein kinase. *Exp. Cell Res.* **179** 554–564

Kasai S, Urushibata S, Hozumi K, *et al*. 2007 Identification of multiple amyloidogenic sequences in laminin-1. *Biochemistry* **46** 3966–3974

Koliakos G, Kouzi-Koliakos K, Triantos A, *et al*. 2000 Laminin-1 phosphorylation by protein kinase A: effect on self assembly and heparin binding. *J. Biochem. Mol. Biol.* **33** 370–378

Koliakos G, Trachana V, Gaitatzi M, *et al*. 2001 Phosphorylation of laminin-1 by protein kinase C. *Mol. Cells* **11** 179–185

Kondrashin A, Nesterova M and Cho-Chung YS 1999 Cyclic adenosine 3′:5′-monophosphate-dependent protein kinase on the external surface of LS-174T human colon carcinoma cells. *Biochemistry* **38** 172–179

Kuratomi Y, Nomizu M, Tanaka K, *et al*. 2002 Laminin γ1 chain peptide, C-16 (KAFDITYVRLKF), promotes migration, MMP-9 secretion and pulmonary metastasis of B16–F10 mouse melanoma cells. *Br. J. Cancer* **86** 1169–1173

Liesi P, Närvänen A, Soos J, *et al*. 1989 Identification of a neurite outgrowth-promoting domain of laminin using synthetic peptides. *FEBS Lett.* **244** 141–148

Machado CF, Beraldo FH, Santos TG, *et al*. 2012 Disease-associated mutations in the prion protein impair laminin-induced process outgrowth and survival. *J. Biol. Chem.* **287** 43777–43788

Mayer U, Nischt R, Pöschl E, *et al*. 1993 A single EGF-like motif of laminin is responsible for high affinity nidogen binding. *EMBO J.* **12** 1879–1885

Mertins P, Yang F, Liu T, *et al*. 2014 Ischemia in tumors induces early and sustained phosphorylation changes in stress kinase pathways but does not affect global protein levels. *Mol. Cell. Proteom*. **13** 1690–1704

Mertins P, Ruggles KV, Gillette MA, *et al*. 2016 Proteogenomics connects somatic mutations to signalling in breast cancer. *Nature* **534** 55–62

Nomizu M, Kuratomi Y, Song SY, *et al*. 1997 Identification of cell binding sequences in mouse laminin γ1 chain by systematic peptide screening. *J. Biol. Chem.* **272** 32198–32205

Olsen JV, Blagoev B, Gnad F, *et al*. 2006 Global, in vivo, and site-specific phosphorylation dynamics in signaling networks. *Cell* **127** 635–648

Ott U, Odermatt E, Engel J, *et al*. 1982 Protease resistance and conformation of laminin. *Eur. J. Biochem.* **123** 63–72

Ponce ML, Nomizu M, Delgado MC, *et al*. 1999 Identification of endothelial cell binding sites on the laminin γ1 chain. *Circ. Res.* **84** 688–694

Pöschl E, Fox JW, Block D, *et al*. 1994 Two non-contiguous regions contribute to nidogen binding to a single EGF-like motif of the laminin gamma 1 chain. *EMBO J.* **13** 3741–3747

Possemato A 2008 CST curation set: 4834; year: 2008; biosample/treatment: cell line, Jurkat/calyculin_A & pervanadate; disease: T cell leukemia; SILAC: -; specificities of antibodies used to purify peptides prior to LCMS: pTXR antibodies used to purify peptides prior to LCMS: phospho-threonine-X-arginine antibody Cat#: 2351, PTMScan(R) phospho-Thr-X-Arg motif (T*XR) immunoaffinity beads Cat#: 1988

Powell SK, Rao J, Roque E, *et al*. 2000 Neural cell response to multiple novel sites on laminin-1. *J. Neurosci. Res.* **61** 302–312

Rakashanda S, Rana F, Rafiq S, *et al*. 2012 Role of proteases in cancer: A review. *Biotechnol. Mol. Biol. Rev.* **7** 90–101

Ren H 2009 CST curation set: 8015; year: 2009; biosample/treatment: tissue, gastrointestinal tract/untreated; disease: gastric cancer; SILAC: -; specificities of antibodies used to purify peptides prior to LCMS: pY antibodies used to purify peptides prior to LCMS: phospho-tyrosine mouse mAb (P-Tyr-100) Cat#: 9411, PTMScan(R) phospho-Tyr motif (Y*) immunoaffinity beads Cat#: 1991

Rigbolt KT, Prokhorova TA, Akimov V, *et al*. 2011 System-wide temporal characterization of the proteome and phosphoproteome of human embryonic stem cell differentiation. *Sci. Signal.* **4** rs3

Rikova K 2011 CST curation set: 10904; year: 2011; biosample/treatment: cell line, NCI-H226/untreated; disease: non-small cell squamous cell lung carcinoma; SILAC: -; specificities of antibodies used to purify peptides prior to LCMS: p[STY]

Ritz-Gold CJ, Cooke R, Blumenthal DK, *et al*. 1980 Light chain phosphorylation alters the conformation of skeletal muscle myosin. *Biochem. Biophys. Res. Commun.* **93** 209–214

Rush J 2008 CST curation set: 4488; year: 2008; biosample/treatment: cell line, MKN-45/untreated & normal; disease: gastric carcinoma; SILAC: -; specificities of antibodies used to purify peptides prior to LCMS: RXXp[ST] antibodies used to purify peptides prior to LCMS: phospho-Akt substrate (RXRXXS/T) (110B7) rabbit mAb Cat#: 9614, PTMScan(R) phospho-Akt substrate motif (RXXS*/T*) immunoaffinity beads Cat#: 1978

Seger D, Gechtman Z and andShaltiel S, 1998 Phosphorylation of vitronectin by casein kinase II: identification of the sites and their promotion of cell adhesion and spreading. *J. Biol. Chem.* **273** 24805–24813

Stokes M 2007 CST curation set: 2262; year: 2007; biosample/treatment: cell line, M059K/UV; disease: glioblastoma; SILAC: -; specificities of antibodies used to purify peptides prior to LCMS: p[ST]Q antibodies used to purify peptides prior to LCMS: phospho-(Ser/Thr) ATM/ATR substrate antibody Cat#: 2851

Streuli CH 1995 Laminin mediates tissue-specific gene expression in mammary epithelia. *J. Cell Biol.* **129** 591–603

The UniProt Consortium 2017 UniProt: the universal protein knowledgebase. *Nucleic Acids Res.* **45** D158–D169

Timpl R, Rohde H, Robey PG, *et al*. 1979 Laminin–a glycoprotein from basement membranes. *J. Biol. Chem.* **254** 9933–9937

Trachana V, Christophorides E, Kouzi-Koliakos K, *et al*. 2005 Laminin-1 is phosphorylated by ecto-protein kinases of monocytes. *Int. J. Biochem. Cell Biol.* **37** 478–492

Verrou KM, Galliou PA, Papaioannou M, *et al*. 2019 Phosphorylation mapping of laminin β1-chain: Kinases in association with functional interaction sequences. *J. Biosci.* **44** 55

Wang H, Li M, Lin W, *et al*. 2007 Extracellular activity of cyclic AMP-dependent protein kinase as a biomarker for human cancer detection: Distribution characteristics in a normal population and cancer patients. *Cancer Epidemiol. Biomarkers Prev.* **16** 789–795

Yalak G and Vogel V 2015 Ectokinases as novel cancer markers and drug targets in cancer therapy. *Cancer Med.* **4** 404–414

Zhou J 2011 CST Curation Set: 12496; Year: 2011; Biosample/Treatment: cell line, Jurkat/calyculin_A & pervanadate; Disease: T cell leukemia; SILAC: -; Specificities of Antibodies Used to Purify Peptides prior to LCMS: pY Antibodies Used to Purify Peptides prior to LCMS: Phospho-Tyrosine Mouse mAb (P-Tyr-100) Cat#: 9411, PTMScan(R) Phospho-Tyr Motif (Y*) Immunoaffinity Beads Cat#: 1991

Zimina EP, Fritsch A, Schermer B, *et al*. 2007 Extracellular phosphorylation of collagen XVII by ecto-casein kinase 2 inhibits ectodomain shedding. *J. Biol. Chem* **282** 22737–22746

Corresponding editor: Ravindra Venkataramani